J Wood Sci (2001) 47:214–220

ORIGINAL ARTICLE

Wook Kang · Hee-Suk Jung

Effects of material constants and geometry on hygrobuckling of wood-based panels

Received: January 17, 2000 / Accepted: June 14, 2000

Abstract To understand and predict hygrobuckling behavior of orthotropic or isotropic wood-based composite panels, the closed form equations were derived using both the displacement function with a double sine series and the energy method under biaxial compressions with an all-clamped-edge condition. The critical moisture content depended on Poisson's ratio (ν) and was inversely proportional to $1 + \nu$ for isotropic panels. It did not depend on the modulus of elasticity (MOE) at all for isotropic panels, but it did depend on MOE ratios for orthotropic panels. As expected, the critical moisture content of plywood was twice as large as the that of hardboard owing to the difference in linear expansions between the two panels. The application of optimum thickness and aspect ratios obtained by the derived equations could improve hygrobuckling resistance without other chemical treatments that could reduce the linear expansion of wood-based panels. This study also indicated that it would be better to increase the aspect ratio rather than the thickness ratio (a/h) from the viewpoint economics.

Key words Hygrobuckling · Orthotropic · Wood-based panel · Aspect/thickness ratio

Introduction

Most furniture panel components are grid structures, and the wood-based panels are fixed on the core with adhesives. Among them, the hollow core type of flush door is one of the most important components, as it is relatively expensive compared to the side, bottom, shelf, and top components. Although the behavior of a wooden flush door due to moisture content change has been studied, most studies have focused on predicting the warping magnitude as the moisture content decreases.[1]

As the availability of quality tropical hardwood for plywood production decreased in recent decades, wood-based composite panels such as medium density fiberboard (MDF), hardboard, and particleboard are being used for the same purpose. One of the problems when using these wood-based composite panels is their surface waviness. This waviness can be observed easily with the naked eye, particularly in the case of doors with surfaces treated with a high-gloss coating. It is believed that the waviness is due to hygrobuckling because of hygroexpansion of the surface. There are few rigorous studies on the hollow core door, and its behaviors are understood qualitatively rather than quantitatively.

For isotropic panels in simply-supported and clamped conditions, the buckling or thermal buckling has been investigated by many researchers for other materials.[2–4] For example, buckling solutions were reported for orthotropic panels in a simply-supported condition under biaxial compression.[5] For all-edges-clamped conditions, Dickinson[6] compared the simple solution with the previous one using Rayleigh's method and beam characteristic function. By contrast, less attention has been paid to the wood-based panel materials developed in relatively recent decades.

In recent years, thermal buckling of laminated composite thick plates has been studied using a finite element method (FEM).[7,8] The authors reported the effects of panel geometries, such as each layer's assembly, thickness ratio, and aspect ratio, on thermal buckling.

Studies on the plate buckling of wood-based panels had been conducted on shearing of the wall when an external force was applied mainly with uniaxial compression,[9,10] but biaxial stress occurs at surfaces via hygroexpansion; hence the relevant equation should be adopted. Spalt and Sutton[11] studied hygrobuckling of strips subjected to a uniaxial compression bar using the equation for critical strain that can be

W. Kang (✉)
Institute of Forestry and Forest Products, College of Agriculture and Life Sciences, Seoul National University, 103 Seodun-Dong, Kwonsun-Gu, Suwon 441-744, Korea
Tel. +82-331-290-2606; Fax +82-331-293-9376
e-mail: kawook53@shinbiro.com

H.-S. Jung
Department of Forest Products, College of Agriculture and Life Sciences, Seoul National University, 103 Seodun-Dong, Kwonsun-Gu, Suwon 441-744, Korea

used without buckling and the magnitude of buckling above the point of critical stress, derived by Suchsland.

The main motivation for this study comes from the need to understand the surface waviness of wood-based composite panels, which can be severe, particularly during summer when they are stored in the yard. It is important to know the critical moisture content where deflection develops rapidly with further hygroexpansion. The hygrobuckling of wood-based panels such as hardboard and plywood has been investigated in only a limited manner. In fact, no standards are available for selecting an optimum distance between cores during manufacture of the hollow core type of flush components.

This study was conducted to look into the effects of the material constants and geometry on hygrobuckling of the hollow core wooden door subjected to biaxial compressive forces as well as buckling by hygroexpansion. In addition, the influence of moisture content changes that can cause buckling was studied for doors made of plywood or hardboard under various conditions.

Theory

The governing equation for the orthotropic buckled plate subjected to in-plane biaxial forces and shear force is given as:

$$D_{11}\frac{\partial^4 w}{\partial x^4} + 2\left(D_{12} + 2D_{66}\right)\frac{\partial^4 w}{\partial x^2 \partial y^2} + D_{22}\frac{\partial^4 w}{\partial y^4} = N_x\frac{\partial^2 w}{\partial x^2} + N_y\frac{\partial^2 w}{\partial y^2} + 2N_{xy}\frac{\partial^2 w}{\partial x \partial y}$$

$$D_{11} = \frac{E_1 h^3}{12(1-\nu_{12}\nu_{21})},\ D_{22} = \frac{E_2 h^3}{12(1-\nu_{12}\nu_{21})},\ D_{12} = D_1\nu_{21},\ D_{66} = \frac{G_{12}h^3}{12} \tag{1}$$

See Appendix for explanation of the abbreviations and symbols.

In this study, only biaxial forces were considered as shown in Fig. 1 because the shear force due to hygroexpansion is not used on wood-based panels such as plywood and hardboard. The energy method was employed to solve Eq. (1).

All-edges-clamped boundary condition

The critical assumption during application of the energy method is the shape of the displacement. Its accuracy depends on the selection of the displacement function. For the all-edges-clamped condition, the displacement function[9,12] can be represented by a double series [Eq. (3)], satisfying the boundary conditions [Eq. (2)].

$$w = dw/dx = 0 \quad \text{for} \quad x = 0,\ a;\ w = dw/dy = 0 \quad \text{for} \quad y = 0, b \tag{2}$$

$$w = \sin\frac{\pi x}{a}\sin\frac{\pi y}{b}\sum_{m=1}^{\infty}\sum_{n=1}^{\infty} a_{mn}\sin\frac{m\pi x}{a}\sin\frac{n\pi y}{b} \tag{3}$$

The buckling mode shape is the same as that of three vibration modes, as shown in Fig. 2. Denoting the work of external forces as ΔT and the strain energy of bending as ΔU gives:

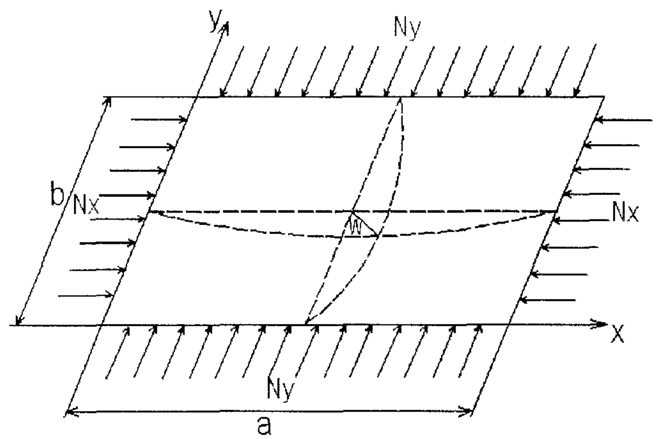

Fig. 1. Coordinate system and dimensions for the biaxial compression condition. See Appendix for abbreviations

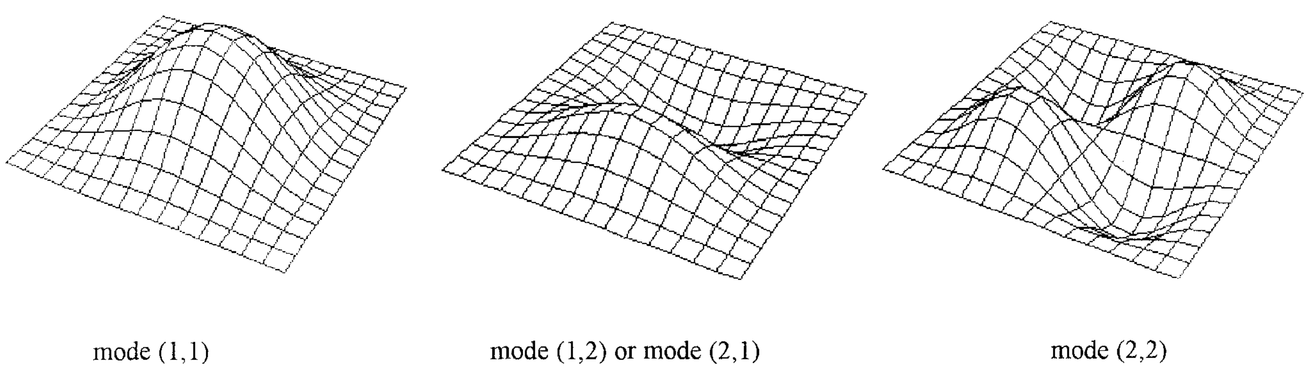

Fig. 2. Buckling mode shapes

$$\Delta U = \frac{1}{2}\int_0^a\int_0^b\left[D_{11}\left(\frac{\partial^2 w}{\partial x^2}\right)^2 + D_{22}\left(\frac{\partial^2 w}{\partial y^2}\right)^2 + 2D_{11}\nu_{21}\frac{\partial^2 w}{\partial x^2}\frac{\partial^2 w}{\partial y^2} + 4D_{66}\left(\frac{\partial^2 w}{\partial x \partial y}\right)^2\right]dxdy \tag{4}$$

$$\Delta T = \frac{1}{2}\int_0^a\int_0^b\left[N_x\left(\frac{\partial w}{\partial x}\right)^2 + N_y\left(\frac{\partial w}{\partial y}\right)^2\right]dxdy$$

Substituting Eq. (3) into Eq. (4), integration by parts leads to Eq. (5). It should be noted that all cross terms are zero due to the orthogonal properties of buckling modes. Therefore,

$$\begin{aligned}\Delta U = \frac{\pi^4}{32}\sum_{m=1}^{\infty}\sum_{n=1}^{\infty}a_{mn}^2\Bigg[&D_{11}\frac{b}{a^3}\left(1 + 6m^2 + m^4\right)\left(1 + \frac{\sin n\pi\cos n\pi}{\pi n\left(n^2 - 1\right)}\right)\\ &+ D_{22}\frac{a}{b^3}\left(1 + 6n^2 + n^4\right)\left(1 + \frac{\sin m\pi\cos m\pi}{\pi m\left(m^2 - 1\right)}\right)\\ &+ 2(\nu_{21}D_{11} + 2D_{66})\frac{\left(n^2 + 1\right)\left(m^2 + 1\right)}{ab}\Bigg]\\ \Delta T = \frac{\pi^2}{32}\sum_{m=1}^{\infty}\sum_{n=1}^{\infty}a_{mn}^2\Bigg[&N_x\frac{b}{a}\left(m^2 + 1\right)\left(1 + \frac{\sin n\pi\cos n\pi}{\pi n\left(n^2 - 1\right)}\right)\\ &+ N_y\frac{a}{b}\left(n^2 + 1\right)\left(1 + \frac{\sin m\pi\cos m\pi}{\pi m\left(m^2 - 1\right)}\right)\Bigg]\end{aligned} \tag{5}$$

Equating ΔT to ΔU, the critical buckling stress by external forces when $m = n = 1$ is expressed as Eq. (6).

$$\left(\sigma_x + \frac{a^2}{b^2}\sigma_y\right)_{\mathrm{cr}} = \frac{4}{3}\frac{\pi^2}{a^2 h}\left[3D_{11} + 2D_{22}\frac{a^4}{b^4} + 2\frac{a^2}{b^2}(\nu_{21}D_{11} + 2D_{66})\right] \tag{6}$$

Equation (6) is the same result as with another solution[2] assuming $D_{11} \cong \nu_{21}D_{11} + 2D_{66}$ for isotropic panels.

For $m = 1$ and $n > 1$, Eq. (6) is expressed as:

$$\left[2\sigma_x + \frac{3}{2}\left(n^2 + 1\right)\frac{a^2}{b^2}\sigma_y\right]_{cr} = \frac{\pi^2}{a^2 h}\left[8D_{11} + \frac{3}{2}\left(n^4 + 6n^2 + 1\right)D_{22}\frac{a^4}{b^4} + 2\left(m^2 + 1\right)\left(n^2 + 1\right)\frac{a^2}{b^2}(\nu_{21}D_{11} + 2D_{66})\right] \tag{7}$$

For $m > 1$ and $n = 1$, Eq. (6) is expressed as:

$$\left[\frac{3}{2}\left(m^2 + 1\right)\sigma_x + 2\frac{a^2}{b^2}\sigma_y\right]_{\mathrm{cr}} = \frac{\pi^2}{a^2 h}\left[\frac{3}{2}\left(m^4 + 6m^2 + 1\right)D_{11} + 8D_{22}\frac{a^4}{b^4} + 2\left(m^2 + 1\right)\left(n^2 + 1\right)\frac{a^2}{b^2}(\nu_{21}D_{11} + 2D_{66})\right] \tag{8}$$

In the case of higher modes, $m > 2$ and $n > 2$, Eq. (6) changes to Eq. (9).

$$\left[\left(m^2 + 1\right)\sigma_x + \left(n^2 + 1\right)\frac{a^2}{b^2}\sigma_y\right]_{\mathrm{cr}} = \frac{\pi^2}{a^2 h}\left[\left(m^4 + 6m^2 + 1\right)D_{11} + \left(n^4 + 6n^2 + 1\right)D_{22}\frac{a^4}{b^4} + 2\left(m^2 + 1\right)\left(n^2 + 1\right)\frac{a^2}{b^2}(\nu_{21}D_{11} + 2D_{66})\right] \tag{9}$$

The relation between stress and hygroexpansion can be represented as Eq. (10).

$$\begin{bmatrix}\sigma_x\\ \sigma_y\end{bmatrix} = \Delta MC\begin{bmatrix}C_{11} & C_{12}\\ C_{21} & C_{22}\end{bmatrix}\begin{bmatrix}-\alpha_x\\ -\alpha_y\end{bmatrix} \tag{10}$$

Therefore,

$$\left(\sigma_x + \frac{a^2}{b^2}\sigma_y\right)_{\mathrm{cr}} = -\Delta MC\left[\left(\alpha_x C_{11} + \alpha_y C_{12}\right) + \frac{a^2}{b^2}\left(\alpha_x C_{21} + \alpha_y C_{22}\right)\right] \tag{11}$$

A critical moisture content (MC_{cr}) can be found by substituting Eq. (11) into Eq. (6).

All edges simply supported boundary condition

Using the same procedures for the edge-clamped condition, the critical buckling stress can be found from Eq. (14) if the displacement function[13] is represented as Eq. (13) in the case of the simply supported condition.

$$w = d^2w/dx^2 = 0 \quad \text{for} \quad x = 0,\ a;\ w = d^2w/dy^2 = 0 \quad \text{for} \quad y = 0, b \tag{12}$$

$$w = \sum_{m=1}^{\infty}\sum_{n=1}^{\infty}a_{mn}\sin\frac{m\pi x}{a}\sin\frac{n\pi y}{b} \tag{13}$$

$$\left(m^2\sigma_x + n^2\frac{a^2}{b^2}\sigma_y\right)_{\mathrm{cr}} = \frac{\pi^2}{a^2 h}\left[m^4 D_{11} + n^4 D_{22}\frac{a^4}{b^4} + 2m^2n^2\frac{a^2}{b^2}(\nu_{21}D_{11} + 2D_{66})\right] \tag{14}$$

Equation (14) is the same as for the other solution.[5]

Experiments

The dry process for hardboard and three-ply lauan plywood panels was selected for test specimens because these panels have been mainly used for furniture: hollow core type flush components (door, side, top, and bottom parts). The adhesive for hardboard and plywood was urea formaldehyde resin. The thickness ratio (a/h) was adjusted as 400:3 because the panel dimensions ($a \times b \times h$) were $460 \times 460 \times 3$ mm. Control specimens for the determination of MOE, dimensional, and moisture content changes were cut along four edges of the buckling specimen (Table 1). Radiata pine laminated veneer lumber (LVL) was used for the core material with dimensions of 26×30 mm. All the specimens cut from the panel were preconditioned at 25°C and 60% relative humidity (RH), but the core specimens were placed indoors and coated with oil-based paint to minimize the effect of dimensional change due to the RH change. The square panels were symmetrically assembled with polyvinyl acetate (PVA) adhesive (Fig. 3) and subjected to the constant humidity chamber where the temperature and RH were 25°C and 90%, respectively. Holes of 8 mm diameter were bored in the middle of the core to reduce the difference in the equilibrium rate between sample panels for buckling and control specimens. Center deflections of the assembled panel were measured at time intervals with a dial gauge.

The analytical solutions for clamped and simply-supported conditions were compared with the results of ANSYS 5.5, a commercial FEM program that has been widely used. The element type and mesh size used were quadilateral 5×5 elements with eight nodes. They were compared with other solutions for thermal or mechanical buckling and experimental results.

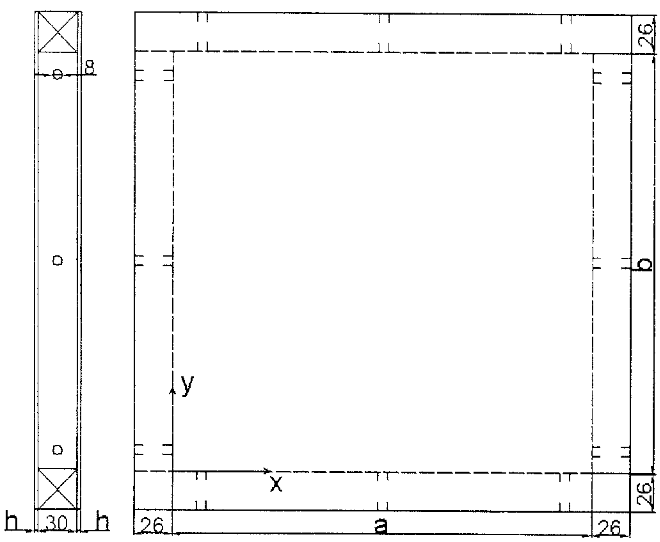

Fig. 3. Specimen geometry and assembly setup for test (units are millimeters)

Results and discussion

Validation of the derived solutions

The derived solutions in this study were compared with results of other studies, as shown in Table 2. There are a few thermal buckling studies, particularly in the case of the all-edges-clamped condition, but the critical temperatures for the isotropic square panel ($a/h = 100$, $\alpha = 2 \times 10^{-3}$, $\nu = 0.3$) were the same exactly. Also, the nondimensional buckling load, $N_x b^2/\pi^2(\nu_{21}D_{11} + 2D_{66})$, for orthotropic panels subjected to uniaxial force [$D_{11}/(\nu_{21}D_{11} + 2D_{66}) = 1.543$, $D_{11}/D_{22} = 0.321$, $N_y = 0$] were a little smaller than Dickinson's

Table 2. Comparison of thermal buckling for isotropic and buckling for orthotropic panels for the all-edges-clamped condition

Loading types	Buckling mode(m,n)	Aspect ratio (a/b)	Buckling load	
			Reference	Present
Isotropic				
Thermal	1,1	1.0	168.71[7]	168.71
Orthotropic				
Mechanical	2,1	1.0	20.74[6] (19.74)[a]	20.45
Uniaxial compression	3,1	1.5	18.34[6] (17.42)[a]	17.77

[a] Values cited from Dickinson[6]

Table 1. Physical and mechanical properties of hardboard and plywood at 25°C, 60% RH

Property	No. of specimens	Hardboard //	Hardboard ⊥	Plywood //	Plywood ⊥
Moisture content (%)	32	6.96 ± 0.36	(10.65 ± 0.44)	10.51 ± 0.28	(13.55 ± 0.32)
Density (g/cm^3)	32	0.93 ± 0.03		0.63 ± 0.02	
Thickness (mm)	32	2.98 ± 0.03	(3.04 ± 0.03)	2.81 ± 0.01	(2.83 ± 0.02)
MOE (GPa)	16	5.06 ± 0.17 (3.55 ± 0.52)	4.89 ± 0.58 (3.65 ± 0.55)	11.86 ± 0.59 (11.55 ± 0.52)	3.53 ± 0.39 (3.22 ± 0.40)
Coefficient of LE ($\times 10^{-3}$)	16	0.380 ± 0.040	0.365 ± 0.047	0.157 ± 0.020	0.155 ± 0.020

Numbers in parentheses are values at equilibrium condition (25°C, 90% RH) ± SD

//, machine or logitudinal direction; ⊥, perpendicular to machine direction; RH, relative humidity; MOE, modulus of elasticity; LE, linear expansion

Table 3. Assumed material constants of plywood and hardboard

Panel	E_1(GPa)	E_2(GPa)	G_{12}(GPa)	ν_{12}	ν_{21}	$\alpha(m/m/\%)$
Plywood	10.0	2.0	0.4	0.12	0.024	0.0002
Hardboard	4.0	4.0	1.6	0.25	–	0.0005

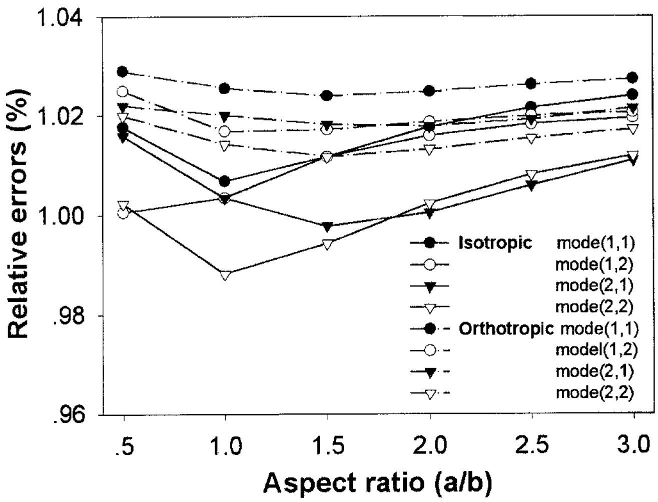

Fig. 4. Comparison of Dickinson's results with present results for isotropic and orthotropic materials by aspect ratios. The relative errors were calculated as the percentage of Dickinson's solution divided by the present solution

value at two modes, but it was slightly larger than other results.[6]

Furthermore, to compare critical moisture contents obtained from this study with other results for different aspect and thickness ratios, material constants for usual hardboard and plywood were assumed as shown in Table 3. In this study, the relative errors of the results were smaller than Dickinson's value with the exception for some modes even though errors depended on material properties and aspect ratios, as shown in Fig. 4. The difference between the present result and those of Dickinson might be attributed to one of the displacement functions assumed. However, the result of this study might be closer to the exact solution than Dickinson's solution because the energy method always causes a slight overestimate compared to that of the exact solutions.

As shown in Tables 4 and 5, the results showed good agreement between the present solutions and the FEM solution when the thickness ratio (a/h) was 100 for both boundary conditions. As expected, critical moisture contents for the clamped condition were about three times larger than those for the simply-supported condition. Moreover, the critical moisture content of plywood was twice as large as that for hardboard owing to the difference in linear expansions between the two panels. For the simply-supported condition, the present solution was slightly larger than the counterpart of the FEM. In contrast, they were smaller than the FEM for the clamped condition except for some cases of plywood. It should be

Table 4. Comparison of critical moisture content in the present solution and the FEM solution for plywood and hardboard for the all-edges-clamped condition at a constant aspect ratio (a/h = 100)

Aspect ratio (a/b)	Plywood		Hardboard	
	Present	FEM	Present	FEM
0.5	1.5476	1.4943	0.5176	0.5368
1.0	1.6729	1.6548	0.7018	0.7386
1.5	2.3341	2.3263	1.2248	1.2714
2.0	3.8354	3.7497	2.0704	2.1182
2.5	5.3747	5.5275	3.2112	3.2484
3.0	7.3658	7.4991	4.6321	4.6433

Results (critical moisture content) are percents
FEM, finite element method

Table 5. Comparison of critical moisture content for the present solution and the FEM solution for plywood and hardboard for the all edges simply-supported condition at a constant aspect ratio (a/h = 100)

Aspect ratio (a/b)	Plywood		Hardboard	
	Present	FEM	Present	FEM
0.5	0.4066	0.3984	0.1625	0.1617
1.0	0.4643	0.4570	0.2632	0.2565
1.5	0.6683	0.6575	0.4277	0.4178
2.0	1.0819	1.0623	0.6580	0.6453
2.5	1.7273[a]	1.6924[a]	0.9541	0.9384
3.0	2.6037[a]	2.5448[a]	1.3159	1.2965

Results (critical moisture content) are percents
[a] Buckling occurred at mode (2,1)

recognized that most of the buckling occurred at mode (1,1), but it was not consistent for orthotropic panels such as plywood as the degrees of orthotropy and aspect ratio increased. This phenomena was compatible with the results for the plywood with aspect ratios of both 2.5 and 3.0 for the all-edges-clamped condition at which buckling occurred at a mode (2,1) in both cases of the present and FEM solutions.

Comparison of analytical solution with experimental results

It is difficult to obtain accurate buckling loads in panels for buckling due to mechanical loading. They are mainly associated with obtaining the desired in-plane loading conditions (e.g., uniform stress), boundary conditions, and the flatness of the panels. In this study, all the equations were derived under the assumptions that the panel is perfectly flat, and the boundary edges are immovable and straight. In practice, wood-based panels have some imperfections,[11] and boundary edges are movable because in-plane stresses act on the boundary edges. The hygrobuckling load or critical moisture content decreases as the degree of imperfection increases,[14,15] whereas it increases as the edge movement increases. In addition, the extent of the edge movement depends on in-plane stresses and panel geometries, including the core ratio.[1] Therefore, the presence of imperfections and the edge movement have combined effects on the buckling behavior when the panels are assembled in the core, which is one of the grid structures. It is not certain whether the boundary condition near surface panels is in a clamped or simply-supported condition even though surface panels of the hollow core door are fixed to the cores with adhesive. It is more likely in the clamped condition as Spalt and Sutton[11] assumed.

By ignoring the presence of imperfections and edge movements, critical moisture contents calculated using Eq. (6) were 0.5% and 1.0% for hardboard and plywood, respectively. It was difficult to control changes in moisture content as much as is required, but the experimental results showed that hygrobuckling occurred when the change of moisture content was less than 2.0% for plywood and less than 1.0% for hardboard, as shown in Fig. 5b.

The above results suggested that the present solutions are accurate for the all-edges-clamped condition. Therefore, the nonparameter hygrobuckling load and critical moisture content of plywood and hardboard were represented for further use as shown in Figs. 6 and 7, respectively.[3]

Equations (6) and (11) show that the critical moisture content depends on Poisson's ratio, and it is inversely proportional to $1 + \nu$ for isotropic panels. It did not depend on the MOE at all for isotropic panels such as hardboard.[4] For orthotropic panels such as plywood, however, it depended on the MOE ratios. It should be noted in the case of plywood that the critical moisture content was much different for different directions even though the aspect ratio was the same (Table 6). To increase the critical moisture content at the same aspect ratio, therefore, the core should be placed perpendicular to the longitudinal direction of plywood.

Conclusions

Based on the displacement function and the energy method, buckling and hygrobuckling equations were derived for orthotropic panels subject to biaxial compression with all edges in both the clamped and simply supported conditions. The following conclusions were derived from this study.

1. Using the displacement function with a double sine series, the results were similar to and simpler than those derived from Dickinson's solution.

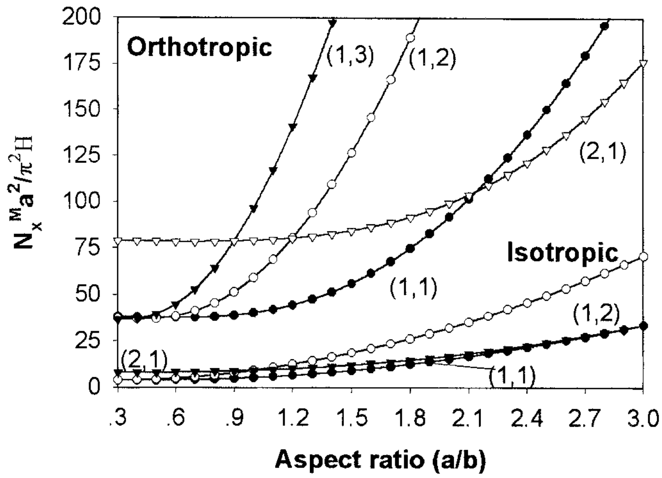

Fig. 6. Nondimensional load parameter of orthotropic and isotropic panels as a function of aspect ratio. $H = V_{21}D_{11} + ZD_{66}$

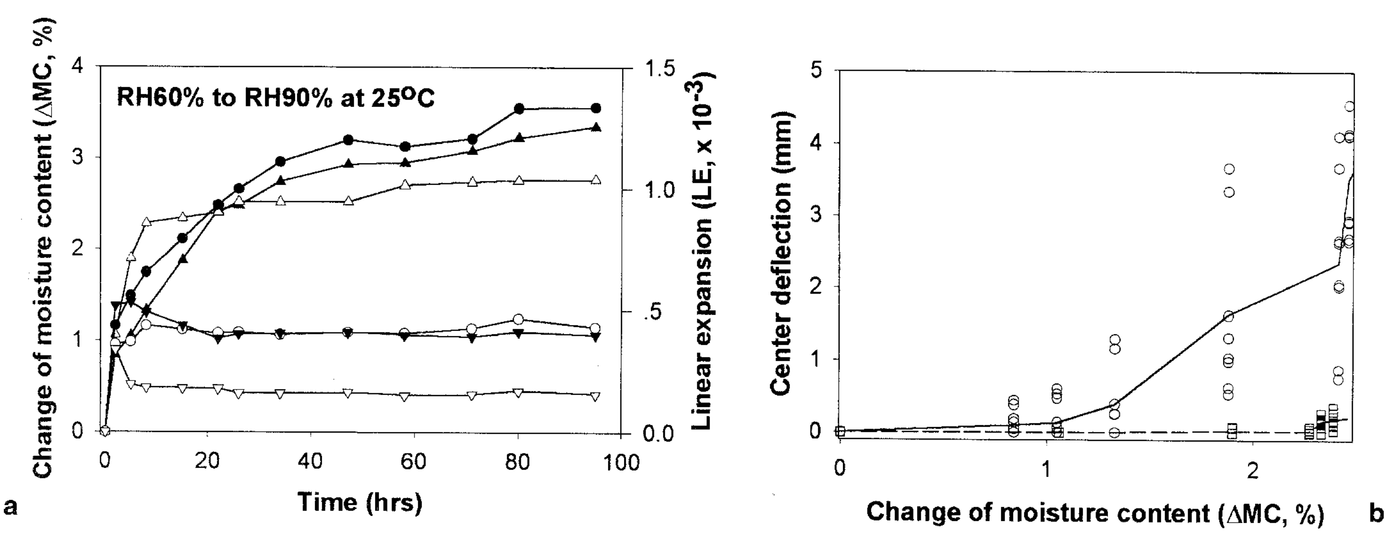

Fig. 5. Percent change of moisture content (ΔMC) and linear expansion (LE) under high relative humidity (RH) conditions (**a**) and center deflection with change of moisture content (**b**). **a** *Solid triangles*, hardboard MC; *open triangles*, plywood MC; *solid circles*, hardboard LE; *open circles*, plywood LE; *solid down triangles*, hardboard LE/MC; *open down triangles*, plywood LE/MC. **b** *Solid line*, hardboard – average; *dashed line*, plywood-average; *open circles*, hardboard – observed; *open squares*, plywood – observed

Table 6. Comparison of critical moisture contents for different directions of panels for the all-edges-clamped condition at the same aspect ratio

Aspect ratio	Plywood	Hardboard
a/*b*		
(*a*/*h* = 100)		
0.3	1.5229	0.5158
3.0	7.3658	4.6321
b/*a*		
(*b*/*h* = 100)		
0.3	0.8146	0.5056
3.0	13.7032	4.6321

Results (critical moisture contents) are percents

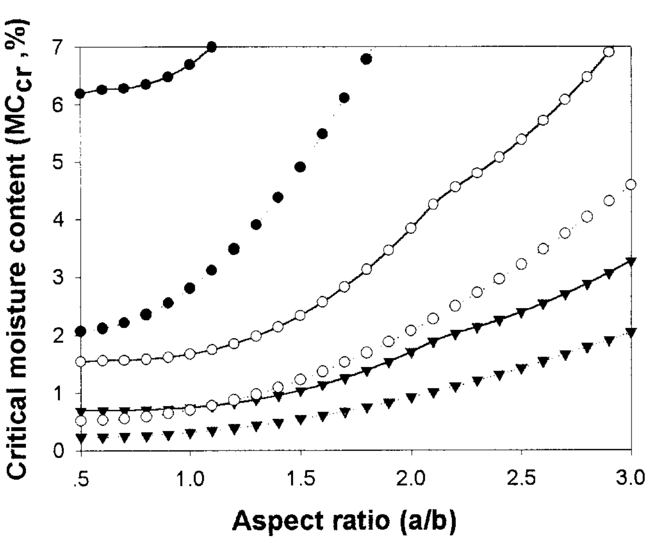

Fig. 7. Changes of critical moisture content (MC_{cr}) by aspect ratio. *Solid lines*, plywood; *dotted lines*, hardboard; *triangles*, *a*/*h* = 150; *open circles*, *a*/*h* = 100; *filled circles*, *a*/*h* = 50

2. The derived equations could be applied to calculate the effects of material constants and the geometry of panels on hygrobuckling by ignoring the presence of imperfections of the panel and the edge movement.
3. The critical moisture content depended on Poisson's ratio and was inversely proportional to $1 + \nu$ for isotropic panels. It did not depend on MOE at all for isotropic panels, whereas it did depend on the MOE ratios for orthotropic panels.
4. The critical moisture content of plywood was twice as large as that for hardboard due to the difference in linear expansions between the two types of panel.
5. Application of the optimum thickness and aspect ratios obtained by the derived equations could improve the hygrobuckling resistance without other chemical treatment to reduce the linear expansion of wood-based panels. It might be better to increase the aspect ratio rather than the thickness ratio (*a*/*h*) from an economical viewpoint. For plywood, core ply should be placed perpendicular to the longitudinal direction.

Appendix: abbreviations and symbols

A_{ij}, D_{ij}	extensional and bending stiffness, respectively
E_i	modulus of elasticity (MOE) in x and y directions, respectively
G_{12}	modulus of rigidity in xy plane
ν_{ij}	Poisson's ratio
h	panel thickness
a, b	panel length in x and y directions, respectively
x, y, z	coordinate system
w	displacement in z direction
ΔMC	moisture content change
α_x, α_y	coefficient of linear expansion in x and y directions, respectively
LE	linear expansion ($\alpha \Delta MC$)
N_x, N_y	resultant in-plane forces per unit length in x and y directions, respectively
N_x^M, N_y^M	hygroscopic forces in x and y directions, respectively

References

1. Kang W, Jung HS (1999) Warping and buckling prediction model of wooden hollow core flush door due to moisture content change (I). Mokchae Konghak, J Korean Wood Sci Technol 27(3):99–116
2. Timoshenko SP, Gere JM (1961) Theory of elastic stability. McGraw-Hill, New York, pp 357, 387
3. Boley BA, Weiner JH (1960) Theory of thermal stresses. Wiley, New York, p 445
4. Hetnarski RB (1986) Thermal stresses I, North Holland, Amsterdam, p 104
5. Ambartsumyan SA, Kunin I (1991) Theory of anisotropic plates. Hemisphere, Washington, DC, p 249
6. Dickinson SM (1978) The buckling and frequency of flexural vibration of rectangular isotropic and orthotropic plates using Rayleigh's method. J Sound Vibration 61(1):1–8
7. Thangaratnam KR, Palaninathan, Ramachandran J (1989) Thermal buckling of composite plates. Comput Struct 32:1117–1124
8. Lee YS, Lee YW, Yang MS, Park BS, Lee JS (1993) Thermal buckling of thick laminated composite plates under uniform temperature distribution. Korean Soc Mech Eng 17:1686–1699
9. Green AE, Hearmon RFS (1945) The buckling of flat rectangular plates: the philosophical magazine. J Theoret Exp Appl Physics 36(7), no. 261
10. Hearmon RFS (1948) The elasticity of wood and plywood. Forest products research special report no. 7. His Majesty's Stationary Office, London
11. Spalt HA, Sutton RF (1968) Buckling of thin surfacing materials due to restrained hygroexpansion. For Prod J 18(4):53–56
12. Chai GB (1994) Buckling of generally laminated composite plates with various edge support conditions. Composite Struct 29:299–310
13. Jones RM (1975) Mechanics of composites materials. Scripta, Washington, DC., p 261
14. Neale KW (1975) Effect of imperfections on elastic buckling of rectangular plates. ASME J Appl Mechan 42:115–120
15. Shen HS (1998) Thermomechanical post-buckling analysis of imperfect laminated plates using a higher order shear-deformation theory. Comput Struct 66:395–409